

# Constructing quasi-equilibrium initial data for binary neutron stars with arbitrary spins

Wolfgang Tichy

*Department of Physics, Florida Atlantic University, Boca Raton, FL 33431, USA*

In general neutron stars in binaries are spinning. Recently, a new quasi-equilibrium approximation that includes a rotational velocity piece for each star has been proposed to describe binary neutron stars with arbitrary rotation states in quasi-circular orbits. We have implemented this approximation numerically for the first time, to generate initial data for neutron star binaries with spin. If we choose the rotational velocity piece such that it equals the Newtonian rigid rotation law, we obtain stars with fluid 4-velocities that have expansion and shear of approximately zero, as one would expect for quasi-equilibrium configurations. We also use the new approach to construct and study initial data sequences for irrotational, corotating and fixed rotation binaries.

PACS numbers: 04.20.Ex, 04.30.Db, 97.60.Jd, 97.80.Fk

## I. INTRODUCTION

Binary neutron stars are at the intersection of two of the most fascinating topics in astrophysics: Gamma ray bursts and gravitational wave astronomy. Binary neutron star mergers (together with black hole neutron star mergers) have been proposed as potential engines for short duration gamma ray bursts [1–8]. These are likely generated in the massive accretion disks around the merger remnant: a larger neutron star or a black hole. In addition, binary neutron star systems are one of the most promising sources for gravitational wave detectors such as LIGO [9, 10], Virgo [11, 12] or GEO [13]. Several of these detectors have been operating over the last few years, while several others are in the planning or construction phase [14]. During the inspiral regime, when the two stars are still well separated they can be well approximated by post-Newtonian theory. Later, when the stars get close, their matter distributions eventually merge together to form a single differentially rotating object. Depending on the total mass, the two progenitors' spins, the equation of state and the strength of magnetic fields this object can either promptly collapse to a black hole, or form a hypermassive neutron star. The hypermassive neutron star is supported against collapse by differential rotation. It can survive for many dynamical timescales, while angular momentum is gradually transported from the inner to the outer parts. Eventually the hypermassive neutron star will also collapse to a black hole surrounded by a massive torus, that is more massive than in the prompt collapse case. Such systems could supply the energy required for a short gamma ray burst [1–6, 8].

In order to make predictions about the last few orbits and the merger of such systems, fully non-linear numerical simulations of the Einstein Equations are required. To start such simulations we need initial data that describe the binary a few orbits before merger. The emission of gravitational waves tends to circularize the orbits [15, 16]. Thus, during the inspiral, we expect the two neutron stars to be in quasi-circular orbits around

each other with a radius that shrinks on a timescale much larger than the orbital timescale. This means that the initial data should have an approximate helical Killing vector  $\xi^\mu$ . In general these neutron stars will be spinning. In the case of the double pulsar PSR J0737-3039 [17] the spin period of the faster spinning star will be  $P_A(t) = 27\text{ms}$  at merger [18] and should thus not be neglected. In the quasi-circular regime the orbital timescale will be much shorter than the spin precession time scale, thus we can assume that the spins are approximately constant.

To incorporate these ideas and to construct numerical initial data for binary neutron stars with arbitrary spins and masses we will use an approach introduced in [18]. In this approach the stars are given spin by choosing a rotational velocity for each star. In this way it is possible to construct stars with both rigid or differential rotation. In equilibrium we of course expect the stars to be rigidly rotating such that the expansion and shear of the fluid 4-velocities of each star vanish. We find that this can be achieved (to good approximation) by setting the rotational velocity of each star equal to the Newtonian rigid rotation law.

We also construct and discuss initial data sequences for irrotational, corotating and fixed rotation binaries.

Spin will have a noticeable effect on the inspiral and merger of the binary if the spin period is within an order of magnitude of the orbital period. Since the orbital period is on the order of a few milliseconds during the late inspiral, we expect interesting spin effects for spin periods on the order of a few dozen milliseconds or less. To date we have observed only ten binary neutron star systems, thus it is not clear yet how likely such spin periods are. Some population synthesis models [19] suggest that radio observable pulsars in neutron star binaries do have a distribution of spin periods that extends down to about 15ms. Other population synthesis models for pulsars [20] come to similar findings. However, since such models involve many parameters that are used to describe sometimes poorly understood physical processes it may be too early to draw definite conclusions about what

spin periods can be expected in neutron star binaries. One parameter that may be of particular importance and that illustrates this uncertainty is the magnetic field decay timescale  $\tau_d$ . In the models it is assumed that the magnetic field of each star decays exponentially on this timescale. Since neutron stars spin down due to magnetic dipole radiation, magnetic field decay can have important effects for the spin down rate and thus the expected spin periods before merger. Unfortunately the value of  $\tau_d$  is controversial. In the first model mentioned [19] the magnetic field decay timescale has to be  $\tau_d \sim 5\text{My}$  in order to fit observations, while in the other model [20] one needs  $\tau_d \sim 2000\text{My}$ .

Throughout we will use units where  $G = c = 1$ . Latin indices such as  $i$  run from 1 to 3 and denote spatial indices, while Greek indices such as  $\mu$  run from 0 to 3 and denote spacetime indices. The paper is organized as follows. Sec. II lists the General Relativistic equations that govern binary spinning neutron stars described by perfect fluids. In Sec. III we briefly describe what algorithm we use to numerically implement these equations. We then present some numerical results in Sec. IV. In particular we describe how one should choose the rotational velocity of each star. We also present particular examples in the form of several initial data sequences. We conclude with a discussion of our method in Sec. V. Some derivations are relegated to the appendices A and B.

## II. BINARY NEUTRON STARS WITH ARBITRARY ROTATION STATES

In this section we briefly describe the equations governing binary neutron stars in arbitrary rotation states in General Relativity. These equations were derived in [18].

We use the Arnowitt-Deser-Misner (ADM) decomposition of Einstein's equations and describe the gravitational fields (i.e. the 4-metric  $g_{\mu\nu}$ ) in terms of the 3-metric  $\gamma_{ij}$ , lapse  $\alpha$ , shift  $\beta^i$  and the extrinsic curvature  $K^{ij}$ . We further assume that the neutron star matter is a perfect fluid with stress-energy tensor

$$T^{\mu\nu} = [\rho_0(1 + \epsilon) + P]u^\mu u^\nu + P g^{\mu\nu}. \quad (1)$$

Here  $\rho_0$  is the mass density (which is proportional the number density of baryons),  $P$  is the pressure,  $\epsilon$  is the internal energy density divided by  $\rho_0$  and  $u^\mu$  is the 4-velocity of the fluid. Assuming a polytropic equation of state

$$P = \kappa \rho_0^{1+1/n} \quad (2)$$

and defining the specific enthalpy

$$h = 1 + \epsilon + P/\rho_0 \quad (3)$$

$\rho_0$ ,  $P$  and  $\epsilon$  can all be expressed in terms of  $h$ . We find

$$\begin{aligned} \rho_0 &= \kappa^{-n} q^n \\ P &= \kappa^{-n} q^{n+1} \\ \epsilon &= nq, \end{aligned} \quad (4)$$

where we have used the abbreviation

$$q = (h - 1)/(n + 1) \quad (5)$$

The fluid 4-velocity  $u^\mu$  is expressed in terms of the 3-velocity

$${}^{(3)}\tilde{u}^i = h\gamma_\nu^i u^\nu, \quad (6)$$

which in turn is split into a irrotational piece  $D^i\phi$  and a rotational piece  $w^i$

$${}^{(3)}\tilde{u}^i = D^i\phi + w^i, \quad (7)$$

where  $D_i$  is the derivative operator compatible with the 3-metric  $\gamma_{ij}$ .

In order to simplify the problem and to obtain elliptic equations we make several assumptions. The first is the existence of an approximate helical Killing vector  $\xi^\mu$ , such that

$$\mathcal{L}_\xi g_{\mu\nu} \approx 0. \quad (8)$$

We also assume similar equations for scalar matter quantities such as  $h$ . For a spinning star, however,  $\mathcal{L}_\xi u^\mu$  is non-zero. Instead we assume that

$$\gamma_i^\nu \mathcal{L}_\xi (\nabla_\nu \phi) \approx 0, \quad (9)$$

so that the time derivative of the irrotational piece of the fluid velocity vanishes in corotating coordinates. We also assume that

$$\gamma_i^\nu \mathcal{L}_{\frac{\nabla_\phi}{h u^0}} w_\nu \approx 0, \quad (10)$$

and

$${}^{(3)}\mathcal{L}_{\frac{w}{h u^0}} w_i \approx 0 \quad (11)$$

which describe the fact that the rotational piece of the fluid velocity is constant along the world line of the star center.

These approximations together with the further assumptions of maximal slicing

$$\gamma_{ij} K^{ij} = 0 \quad (12)$$

and conformal flatness

$$\gamma_{ij} = \psi^4 \delta_{ij} \quad (13)$$

yield the following coupled equations:

$$\bar{D}^2 \psi + \frac{\psi^5}{32\alpha^2} (\bar{L}B)^{ij} (\bar{L}B)_{ij} + 2\pi\psi^5 \rho = 0, \quad (14)$$

$$\bar{D}_j (\bar{L}B)^{ij} - (\bar{L}B)^{ij} \bar{D}_j \ln(\alpha\psi^{-6}) - 16\pi\alpha\psi^4 j^i = 0, \quad (15)$$

$$\bar{D}^2(\alpha\psi) - \alpha\psi \left[ \frac{7\psi^4}{32\alpha^2} (\bar{L}B)^{ij} (\bar{L}B)_{ij} + 2\pi\psi^4(\rho + 2S) \right] = 0, \quad (16)$$

$$D_i \left[ \frac{\rho_0 \alpha}{h} (D^i \phi + w^i) - \rho_0 \alpha u^0 (\beta^i + \xi^i) \right] = 0, \quad (17)$$

and

$$h = \sqrt{L^2 - (D_i \phi + w_i)(D^i \phi + w^i)}. \quad (18)$$

Here  $(\bar{L}B)^{ij} = \bar{D}^i B^j + \bar{D}^j B^i - \frac{2}{3} \delta^{ij} \bar{D}_k B^k$ ,  $\bar{D}_i = \partial_i$ , and we have introduced

$$B^i = \beta^i + \xi^i + \Omega \epsilon^{ij3} (x^j - x_{CM}^j), \quad (19)$$

$$\begin{aligned} \rho &= \alpha^2 [\rho_0 (1 + \epsilon) + P] u^0 u^0 - P, \\ j^i &= \alpha [\rho_0 (1 + \epsilon) + P] u^0 u^0 (u^i / u^0 + \beta^i), \\ S^{ij} &= [\rho_0 (1 + \epsilon) + P] u^0 u^0 (u^i / u^0 + \beta^i)(u^j / u^0 + \beta^j) \\ &\quad + P \gamma^{ij}, \end{aligned} \quad (20)$$

$$\begin{aligned} u^0 &= \frac{\sqrt{h^2 + (D_i \phi + w_i)(D^i \phi + w^i)}}{\alpha h}, \\ L^2 &= \frac{b + \sqrt{b^2 - 4\alpha^4 [(D_i \phi + w_i)w^i]^2}}{2\alpha^2}, \\ b &= [(\xi^i + \beta^i)D_i \phi - C]^2 + 2\alpha^2 (D_i \phi + w_i)w^i, \end{aligned} \quad (21)$$

where we sum over repeated spatial indices irrespective of whether they are up or down and where  $C$  is a constant of integration that in general has a different value inside each star. Below we will denote these two values by  $C_+$  and  $C_-$ . Notice that in an inertial frame the approximate helical Killing vector has the components

$$\xi^\mu = (1, -\Omega[x^2 - x_{CM}^2], \Omega[x^1 - x_{CM}^1], 0). \quad (22)$$

Here  $x_{CM}^i$  denotes the center of mass position of the system, and  $\Omega$  is the orbital angular velocity, which we have chosen to lie along the  $x^3$ -direction.

The elliptic equations (14), (15), (16) and (17) above have to be solved subject to the boundary conditions

$$\lim_{r \rightarrow \infty} \psi = 1, \quad \lim_{r \rightarrow \infty} B^i = 0, \quad \lim_{r \rightarrow \infty} \alpha \psi = 1 \quad (23)$$

at spatial infinity, and

$$(D^i \phi) D_i \rho_0 + w^i D_i \rho_0 = h u^0 (\beta^i + \xi^i) D_i \rho_0 \quad (24)$$

at each star surface. Note that the rotational piece of the fluid velocity  $w^i$  can be freely chosen.

Once the equations (14), (15), (16), (17) and (18) are solved we know  $h$  (and thus the matter distribution) and the fluid 3-velocity  $^{(3)}\tilde{u}^i$  via Eq. (7). The 3-metric is obtained from Eq. (13) and the extrinsic curvature is given by

$$K^{ij} = \frac{1}{2\psi^4 \alpha} (\bar{L}\beta)^{ij}. \quad (25)$$

Notice that Eq. (18) can also be written as

$$\begin{aligned} \ln h + \frac{1}{2} \ln \left[ \alpha^2 - \left( \beta^i + \xi^i + \frac{w^i}{h u^0} \right) \left( \beta_i + \xi_i + \frac{w_i}{h u^0} \right) \right] \\ = -\ln \Gamma + \ln(-C), \end{aligned} \quad (26)$$

where we have introduced

$$\begin{aligned} \Gamma = u^0 \sqrt{\left[ \alpha^2 - \left( \beta^i + \xi^i + \frac{w^i}{h u^0} \right) \left( \beta_i + \xi_i + \frac{w_i}{h u^0} \right) \right]} \\ \times \left( 1 - \left( \beta^i + \xi^i + \frac{w^i}{h u^0} \right) \frac{D_i \phi}{\alpha^2 h u^0} - \frac{w_i w^i}{(\alpha h u^0)^2} \right). \end{aligned} \quad (27)$$

Our approach, while more general, has certain similarities with the approach in [21, 22], hereafter BS. For example our Eq. (7) reduces to Eq. (52) of BS if we assume  $w^i = \eta \xi^i$ . Furthermore, using the approximations in Eqs. (9), (10) and (11), we are able to find the first integral (18) of the Euler equation. This means that within our approximations the Euler equation has vanishing curl. That is precisely what has to hold if the approach in BS (which converts the Euler equation into an elliptic equation by taking its divergence) is to succeed. The problem with the BS approach is that it simply assumes  $\mathcal{L}_\xi \tilde{u}^\mu = 0$  instead of our Eqs. (9), (10) and (11). This leads to extra terms in the Euler equation, which cause a non-vanishing curl. Thus, the BS approach is not entirely consistent since it requires zero curl of the Euler equation, while at the same time it uses an Euler equation with non-vanishing curl. Furthermore, the boundary condition given by BS for their new elliptic equation has to be imposed at the star surface. Since the location of the star surface is another unknown function one needs an equation or an algorithm to determine this location. No such algorithm is given by BS. The usual iterative approach where we simply search for the surface where  $h = 1$  in each iteration (see e.g. Sec. III) will not work, because the boundary condition given by BS ensures that  $h = 1$  occurs at the surface where we impose their boundary condition. So in this kind of iterative procedure the star surface would always remain at the location of the initial guess for the surface.

### III. NUMERICAL METHOD

To construct initial data we have to solve the elliptic equations (14), (15), (16) and (17) together with the algebraic equation (18). This set of equations has a similar structure as for the well known case of irrotational neutron star binaries, which has been solved before [23–31]. In this work we will use the SGRID code [32–34], which uses pseudospectral methods to accurately compute spatial derivatives. We use the same decomposition into 6 domains as was used in [33] for the case of corotating neutron star binaries. In this approach one star center is put on the positive and the other on the negative  $x$ -axis. Then complicated coordinate transformations are used to transform from Cartesian like coordinates  $(x, y, z)$  to new coordinates  $(A, B, \varphi)$ . Here the coordinates  $A$  and  $B$  both range from 0 to 1, and  $\varphi$  is a polar angle measured around the  $x$ -axis. The actual coordinate transformations are different in each domain. This results in two domains that cover the outside of each star (including

spatial infinity) for either  $x \geq 0$  or  $x \leq 0$ . These two domains touch at  $x = 0$ . Since they contain spatial infinity it is trivial to impose the boundary conditions in Eq. (23). The coordinate transformations contain freely specifiable functions  $\sigma_{\pm}(B, \varphi)$  so that one can always make the inner domain boundaries coincide with the star surfaces. The inside of each star is covered by two more domains. One of these stretches from the star surface up to a certain depth inside the star. The other covers the remainder of the star interior. The elliptic equations (14), (15) and (16) need to be solved in all domains, while the matter equations (17) and (18) are solved only inside each star. Two of the domain boundaries always coincide with the neutron star surfaces so that it is straightforward to impose the boundary condition (24) for  $\phi$  at each star surface. Notice, however, that Eq. (17) and its boundary condition in Eq. (24) do not uniquely specify a solution  $\phi$ . If  $\phi$  solves both Eqs. (17) and (24)  $\phi + \text{const}$  will be a solution as well. In order to obtain a unique solution we modify the boundary condition by adding the volume integral  $\int_{\text{star}} \phi dV$  over the star interior to the left hand side of Eq. (24). Furthermore, in the domains covered by the  $A, B, \varphi$  coordinates we impose the following regularity conditions along the  $x$ -axis:

$$\partial_{\varphi}\Psi = 0, \quad \partial_s\Psi + \partial_s\partial_{\varphi}\partial_{\varphi}\Psi = 0, \quad (28)$$

where  $\Psi$  stands for either  $\psi$ ,  $B^i$ ,  $\alpha$  or  $\phi$ , and  $s = \sqrt{y^2 + z^2}$  is the distance from the  $x$ -axis.

In order to solve the elliptic equations (14), (15), (16) and (17) we need a fixed domain decomposition. However, the location of the star surfaces (where  $h = 1$ ) is not a priori known, but rather determined by Eq. (18). For this reason we use the following iterative procedure:

1. We first come up with an initial guess for  $h$  in each star, in practice we simply choose Tolman-Oppenheimer-Volkoff solutions (see e.g. Chap. 23 in [35]) for each. For the irrotational velocity potential we choose  $\phi = \Omega(x_{C*}^1 - x_{CM}^1)x^2$ , where  $x_{C*}^1$  and  $x_{CM}^1$  is the center of the star and the center of mass. We choose the initial orbital angular velocity according to post-Newtonian theory.
2. We then evaluate the residuals [i.e. the  $L^2$ -norm of the left hand sides of Eqs. (14), (15), (16) and (17)]. If the combined residual is below a prescribed tolerance we are done and exit the iteration at this point.
3. If the residual of Eq. (17) is larger than 10% of the combined residuals of Eqs. (14), (15) and (16), we solve Eq. (17) for  $\phi$ . We then reset  $\phi$  to  $\phi = 0.2\phi_{\text{ell}} + 0.8\phi_{\text{old}}$ , where  $\phi_{\text{ell}}$  is the just obtained solution of Eq. (17) and  $\phi_{\text{old}}$  is the previous value of  $\phi$ .
4. Next we solve the 5 coupled elliptic equations (14), (15) and (16) for  $\Psi_{\text{ell}} = (\psi, B^i, \alpha)_{\text{ell}}$ . We then set  $\Psi = (\psi, B^i, \alpha)$  to  $\Psi = 0.4\Psi_{\text{ell}} + 0.6\Psi_{\text{old}}$ .

5. In order to also solve Eq. (18) we need to know the values of the constants  $C_{\pm}$  in each star as well as  $\Omega$  and  $x_{CM}^1$ . We first determine the star centers  $x_{C*\pm}^1$  by finding the maximum of the current  $h$  along the  $x$ -axis. Since the location of each star center is given by  $\partial_1 h|_{x_{C*\pm}^1} = 0$ , Eq. (26) [which is equivalent to Eq. (18)] yields

$$\partial_1 \ln \left[ \alpha^2 - \left( \beta^i + \xi^i + \frac{w^i}{hu^0} \right) \left( \beta_i + \xi_i + \frac{w_i}{hu^0} \right) \right] \Big|_{x_{C*\pm}^1} = -2\partial_1 \ln \Gamma \Big|_{x_{C*\pm}^1} \quad (29)$$

Note that  $\beta^i + \xi^i$  is a function of  $\Omega$  and  $x_{CM}^1$ . We now update  $\Omega$  and  $x_{CM}^1$  by solving Eq. (29) for  $\Omega$  and  $x_{CM}^1$  so that the star centers  $x_{C*\pm}^1$  remain in the same location, when we update  $h$  according to Eq. (18) or Eq. (26). For this reason Eq. (29) is sometimes referred to as force balance equation. One noteworthy caveat is that we evaluate the derivative of  $\ln \Gamma$  in Eq. (29) for the  $\Omega$  and  $x_{CM}^1$  before the update. Since we iterate over these steps this approximation does not introduce any errors. However, it is essential for the overall stability of our iterative procedure.

6. Next, we use Eq. (18) to update  $h$  in each star, while at the same time adjusting  $C_{\pm}$  such that the rest mass of each star remains constant. This update is numerically expensive because the domain boundaries need to be adjusted (by changing  $\sigma_{\pm}(B, \varphi)$ ) such that they remain at the star surfaces, which change whenever  $h$  is updated. When we adjust  $\sigma_{\pm}(B, \varphi)$  it can be helpful for the stability of the overall iteration to filter out high frequency modes in  $\sigma_{\pm}(B, \varphi)$  and to impose  $\partial_B \sigma_{\pm}(B, \varphi)|_{B=0,1} = 0$ . The latter keeps the stars from drifting away from the  $x$ -axis during the iterations.
7. Finally we go back to step 2.

## IV. NUMERICAL RESULTS

We have implemented the method described above in the SGRID code [32–34]. In this section we present some numerical results using this code. All our results are presented in units where  $G = c = \kappa = 1$  and we only use  $n = 1$  in the polytropic equation of state.

### A. Choice of rotational velocity piece $w^i$

As already mentioned we hold the rest masses fixed during the iterations described in Sec. III. Similarly we need to fix the rotational velocity piece  $w^i$  that gives rise to the spin in each star. Ideally we would like to

choose  $w^i$  such that the expansion and shear of the fluid are approximately zero. As we show in Appendices A and B, this is true if the velocity in the corotating frame  $V^\mu = u^\mu/u^0 - \xi^\mu$  is of the form

$$V^i = \epsilon^{ijk} \hat{\omega}^j [x^k - x_{C*}^k(t)]. \quad (30)$$

where  $x_{C*}^k$  is the location of the star center, which could be defined as the point with the highest rest mass density  $\rho_0$  or as the center of mass of the star. Thus our task is to choose  $w^i$  such that Eq. (30) holds. In [18] we have speculated that a good choice might be  $D_i w^i = 0$ , which can be rewritten in terms of the derivative operator  $\bar{D}_i = \partial_i$  as  $\bar{D}_i \bar{w}^i = 0$  if we introduce

$$\bar{w}^i = \psi^6 w^i. \quad (31)$$

It is clear that

$$\bar{w}^i = f(|x^n - x_{C*}^n|) \epsilon^{ijk} \omega^j (x^k - x_{C*}^k), \quad (32)$$

satisfies  $\bar{D}_i \bar{w}^i = 0$  for any function  $f(|x^n - x_{C*}^n|)$  that only depends on the conformal distance from the star's center. We have tested the simplest case of  $f = 1$ , and find that the  $V^i$  that results from this choice after solving all equations is similar to Eq. (30) but with a position dependent  $\hat{\omega}^j$ , so that we have differential rotation in the star which leads to non-zero shear. Another simple choice is

$$\bar{w}^i = \psi^6 \epsilon^{ijk} \omega^j (x^k - x_{C*}^k). \quad (33)$$

Numerically, we find that this choice results in a  $V^i$  that is very close to the form in Eq. (30). In Fig. 1 we show results for an unequal mass system where both stars have  $\bar{w}^i$  as in Eq. (33) with  $\omega^i = (0, 0, 0.025)$ . Since  $V^i$  varies linearly with  $x^i$  we see that it is of the form in Eq. (30). The slope of  $V^i$  corresponds to  $\hat{\omega}^i \approx (0, 0, -0.015)$ , so that we obtain  $\omega^i \approx \Omega^i + \hat{\omega}^i$ , which would hold exactly in Newtonian theory.

### B. Initial data sequences

In order to test our method we have performed simulations with different rotation states. In Figs. 2 and 3 we show how the ADM mass  $M_{ADM}$  and the ADM angular momentum  $J_{ADM}$  vary as a function of the orbital angular velocity  $\Omega$  for a binaries with rest masses  $m_{01} = 0.1461$  and  $m_{02} = 0.1299$ . Note that increasing  $\Omega$  corresponds to decreasing separation. As we can see our numerical results (pluses, stars and crosses) approach the expected post-Newtonian results (taken from [36–39]) for non-spinning point particles (solid line) for small  $\Omega$ . In fact we find that the results for irrotational ( $w^i = 0$ ) stars (marked by stars in Figs. 2 and 3) agree very well with post-Newtonian non-spinning point particle results for all  $\Omega$  we have investigated. On the other hand, for corotating binaries (pluses) we obtain larger  $M_{ADM}$  and  $J_{ADM}$  values, especially for larger  $\Omega$ , which is expected

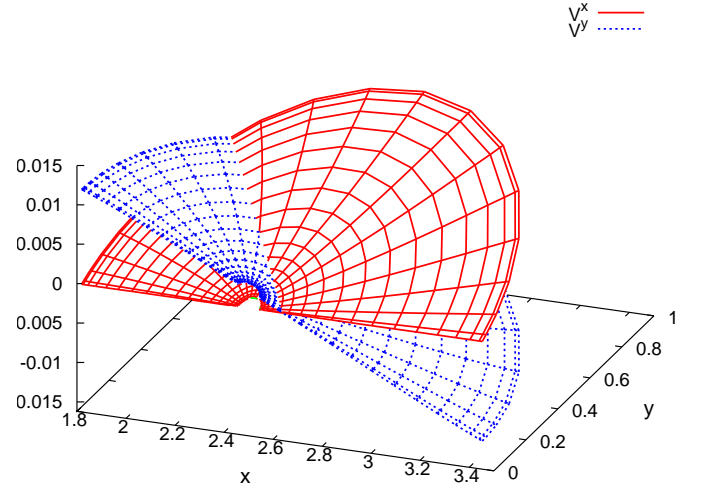


FIG. 1: The Cartesian  $x$ - and  $y$ -components of  $V^i$  in the orbital plane of a the star with rest mass  $m_{01} = 0.1461$ . The other star has rest mass  $m_{02} = 0.1299$ . The separation between both star centers is  $D = 5.2885$ , which corresponds to an orbital angular velocity of  $\Omega = 0.03928$ . Both stars' rotational velocity piece is given by Eq. (33) with  $\omega^i = (0, 0, 0.025)$ . We see that both  $V^x$  and  $V^y$  vary linearly and thus obey Eq. (30).

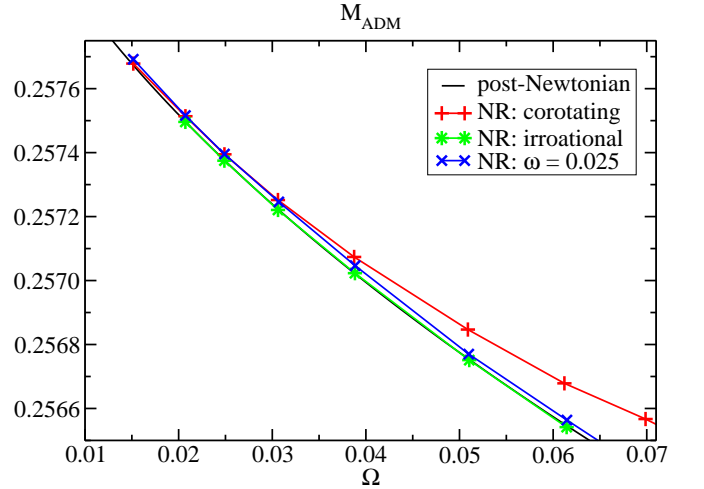


FIG. 2: The ADM mass for a binary with rest masses  $m_{01} = 0.1461$  and  $m_{02} = 0.1299$  as a function of orbital angular velocity. Shown are results for post-Newtonian point particles (solid line), and three different numerical results (NR) for corotating stars (pluses), irrotational stars (marked by stars), and a case where both stars have spin (crosses) with  $\omega^i = (0, 0, 0.025)$ .

because to maintain corotation the stars have to spin more for higher  $\Omega$ . Finally, we have also investigated the case of a binary where both stars have the same constant rotational velocity  $w^i = \epsilon^{ijk} \omega^j (x^k - x_{C*}^k)$  with  $\omega^i = (0, 0, 0.025)$ . This  $\omega^i$  corresponds to a spin period of 14ms [for  $\kappa = 0.018 \text{m}^5/(\text{kg s}^2)$ ]. In Figs. 2 and 3 this case is denoted by crosses. Since here the stars

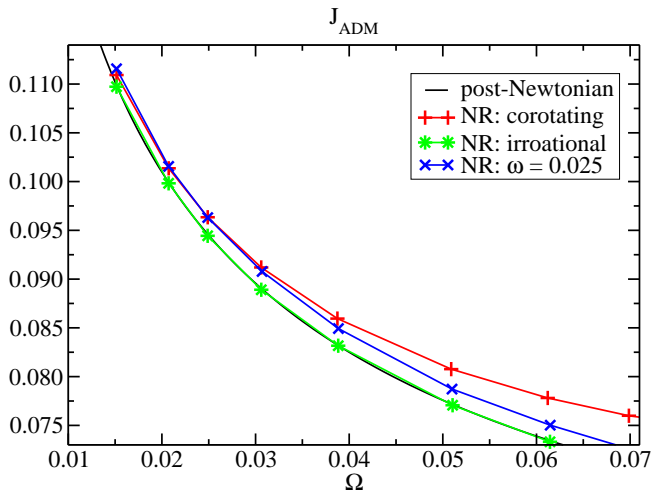


FIG. 3: The ADM angular momentum for the same binaries as in Fig. 2.

always have rotational velocity we obtain larger  $M_{ADM}$  and  $J_{ADM}$  values than in the irrotational case for all  $\Omega$ . However, since the rotational velocity is always the same we get less  $M_{ADM}$  and  $J_{ADM}$  than in the corotating case (pluses) for large  $\Omega$ , and more  $M_{ADM}$  and  $J_{ADM}$  than in the corotating case (pluses) for small  $\Omega$ .

## V. DISCUSSION

Realistic neutron stars in binaries are spinning. From observations of millisecond pulsars we know that these spins can be substantial enough to influence the late inspiral and merger dynamics of the binary. The spins might also influence the lifetime of an angular momentum supported hypermassive neutron star that can form after merger. With more angular momentum we expect the hypermassive star to survive for longer. This can have important consequences for both the gravitational waves emitted by the system and also for the likelihood of a gamma ray burst.

The purpose of this paper is to numerically implement and test a new method for the computation of binary neutron star initial data with arbitrary rotation states. This method is derived from the standard matter equations of perfect fluids together with certain quasi-equilibrium assumptions. We assume that there is an approximate helical Killing vector  $\xi^\mu$  and that Lie derivatives of the metric variables with respect to  $\xi^\mu$  vanish. We also assume that scalar matter variables such as  $h$  or  $\rho_0$  have Lie derivatives that vanish with respect to  $\xi^\mu$ . However, since the Lie derivative of the fluid velocity  $u^\mu$  is non-zero for generic spins, we split the fluid velocity  $u^\mu$  into an irrotational piece (derived from a potential  $\phi$ ) and a rotational piece  $w^i$ , and assume that only the irrotational piece has a vanishing Lie derivative (see Eq. (9)) with respect to  $\xi^\mu$ . Furthermore we know that the spin of each

star remains approximately constant since the viscosity of the stars is insufficient for tidal coupling [40]. To incorporate this fact, we use Eqs. (10) and (11) which are based on the assumption that  $w^i$  is constant along the star's motion described by the irrotational velocity piece  $\nabla^\mu \phi$ .

From these assumptions we obtain the elliptic equations (14), (15), (16) and (17) together with the algebraic equation (18). The specific enthalpy  $h$  in Eq. (18) determines the shape of the star surfaces. Since our elliptic solvers work on a fixed domain decomposition where the star surfaces have to coincide with domain boundaries we solve this mixture of elliptic and algebraic equations by iteration. In each iteration we first solve the elliptic equations for a given  $h$  and then use the algebraic Eq. (18) to update  $h$ . The stability of this iterative procedure is improved if we do the following. (A) We typically do not take the  $\psi$ ,  $B^i$  and  $\alpha$  and  $\phi$  coming from solving Eqs. (14), (15), (16) and (17) as our new fields. Rather, we take the average of this solution and the values from the previous iteration step as our new fields. In this way  $\psi$ ,  $B^i$  and  $\alpha$  and  $\phi$  change less from one iteration step to the next. (B) We use the force balance condition as given in Eq. (29) to update  $\Omega$  and  $x_{CM}^1$ .

For each iteration we also need to specify rotational piece  $w^i$  of the fluid velocity. We have found that the choice in Eq. (33) works very well in the sense that after numerically solving all equations it leads to a velocity in the corotating frame of the form  $\vec{V} = \vec{\omega} \times \vec{r}$  as in Eq. (30). In Appendices A and B we show that this form of  $\vec{V}$  results in a fluid 4-velocity with an expansion and shear that are approximately zero, as we would expect for stars in equilibrium. This means that we have found a simple way to generate initial data for neutron star binaries that ensure that the stars are spinning and without differential rotation.

We also compare initial data sequences for irrotational, corotating and fixed rotation binaries. We find that our method yields reasonable results. All sequences approach post-Newtonian results for large separations. And the binary sequences with fixed rotation yield higher  $M_{ADM}$  and  $J_{ADM}$  than corotating configurations for large separations, and lower  $M_{ADM}$  and  $J_{ADM}$  than corotating configurations for small separations.

## Acknowledgments

It is a pleasure to thank Sebastiano Bernuzzi for helpful discussions. This work was supported by NSF grants PHY-0855315 and PHY-1204334.

### Appendix A: Expansion, shear and rotation of the fluid

If  $u^\mu$  denotes the 4-velocity of the fluid we can split its derivatives into

$$\nabla_\nu u_\mu = \frac{1}{3}\Theta P_{\mu\nu} + \sigma_{\mu\nu} + \omega_{\mu\nu} - a_\mu u_\nu, \quad (\text{A1})$$

where

$$P_{\mu\nu} = g_{\mu\nu} + u_\mu u_\nu, \quad (\text{A2})$$

and where the expansion, shear, rotation and acceleration are defined as

$$\Theta = P^{\mu\nu} \nabla_\mu u_\nu, \quad (\text{A3})$$

$$\sigma_{\mu\nu} = P_\mu^{\mu'} P_\nu^{\nu'} \nabla_{(\mu'} u_{\nu')} - \frac{1}{3}\Theta P_{\mu\nu}, \quad (\text{A4})$$

$$\omega_{\mu\nu} = P_\mu^{\mu'} P_\nu^{\nu'} \nabla_{[\nu'} u_{\mu']} \quad (\text{A5})$$

and

$$a_\mu = u^\nu \nabla_\nu u_\mu. \quad (\text{A6})$$

If the 4-velocity is of the form

$$u^\mu = f \bar{u}^\mu, \quad (\text{A7})$$

where  $f$  is any scalar function, it immediately follows (from  $P_{\mu\nu} u^\nu = 0$ ) that

$$\Theta = f P^{\mu\nu} \nabla_\mu \bar{u}_\nu, \quad (\text{A8})$$

$$\sigma_{\mu\nu} = f P_\mu^{\mu'} P_\nu^{\nu'} \nabla_{(\mu'} \bar{u}_{\nu')} - \frac{1}{3}\Theta P_{\mu\nu}, \quad (\text{A9})$$

and

$$\omega_{\mu\nu} = f P_\mu^{\mu'} P_\nu^{\nu'} \nabla_{[\nu'} \bar{u}_{\mu']}. \quad (\text{A10})$$

For our purposes it is often convenient to write the 4-velocity as

$$u^\mu = u^0(\xi^\mu + V^\mu), \quad (\text{A11})$$

where in an inertial frame the helical Killing vector is given by Eq. (22) and  $u^0 = -n_\mu u^\mu / \alpha$ . Note that  $\xi^0 = 1$  leads to  $V^0 = 0$ . From

$$\frac{dx^\mu}{dt} = \frac{u^\mu}{u^0} = \xi^\mu + V^\mu \quad (\text{A12})$$

we see that  $V^\mu$  can be interpreted as the velocity in the corotating frame.

The fact that  $\nabla_{(\mu} \xi_{\nu)} = 0$  together with Eqs (A8) and (A9) yields

$$\Theta = u^0 P^{\mu\nu} \nabla_\mu V_\nu, \quad (\text{A13})$$

and

$$\sigma_{\mu\nu} = u^0 P_\mu^{\mu'} P_\nu^{\nu'} \nabla_{(\mu'} V_{\nu')} - \frac{1}{3}\Theta P_{\mu\nu}. \quad (\text{A14})$$

Thus we see that if we have  $\nabla_{(\mu} V_{\nu)} \approx 0$ , the expansion and shear are approximately zero.

### Appendix B: Expansion and shear if $\vec{V} = \vec{\omega} \times \vec{r}$

Let us assume that  $V^\mu = (0, V^i)$  is given by Eq. (30). Let us further assume that  $V^i$  is small in the sense that

$$V^i \sim O(\epsilon) \quad (\text{B1})$$

with  $\epsilon \ll 1$ . We know (e.g. from post-Newtonian theory) that the shift is also small. For simplicity we assume that

$$\beta^i \sim O(\epsilon). \quad (\text{B2})$$

Using  $\nabla_{(\mu} V_{\nu)} = \mathcal{L}_V g_{\mu\nu}/2$  and Eq. (13) we then find

$$\begin{aligned} \nabla_{(0} V_{0)} &= -V^i \partial_i \alpha + O(\epsilon^2) \\ \nabla_{(0} V_{i)} &= O(\epsilon^2) \\ \nabla_{(i} V_{j)} &= 2\psi^3 V^i \partial_i \psi \delta_{ij}. \end{aligned} \quad (\text{B3})$$

Recall that the Newtonian potential near a mass  $m_1$  is given by

$$U \approx \frac{m_1}{r} + \frac{m_2}{D} \left( 1 + \frac{x^1 - x_{C*}^1(t)}{D} \right), \quad (\text{B4})$$

where  $m_2$  is a second mass at a distance  $D$  in the  $x$ -direction. Since  $\psi \propto U$  and  $\alpha \propto U$  we find that

$$V^i \partial_i \psi \sim V^i \partial_i \alpha \sim O(\epsilon^3), \quad (\text{B5})$$

where we have used the virial theorem and set  $\frac{m_2}{D} = O(\epsilon^2)$ .

From  $u_\mu u^\mu = -1$  we obtain

$$u^0 = \frac{1}{\alpha} + O(\epsilon^2), \quad (\text{B6})$$

which leads us to

$$P^{\mu\nu} = \gamma^{\mu\nu} + O(\epsilon^2). \quad (\text{B7})$$

From Eqs (A13), (A14), (B3), (B5) and (B7) we see that

$$\Theta = \sigma_{\mu\nu} = O(\epsilon^3) \quad (\text{B8})$$

if  $V$  is of the form  $\vec{\omega} \times \vec{r}$  as in Eq. (30). This means that expansion and shear for this particular  $V^i$  are smaller by a factor of  $O(\epsilon^2)$  than for a generic  $V^i$ .

- 
- [1] R. Narayan, B. Paczynski, and T. Piran, *Astrophys. J.* **395**, L83 (1992).
  - [2] T. Piran, *Phys.Rept.* **333**, 529 (2000), astro-ph/9907392.
  - [3] T. Piran, *Phys.Rept.* **314**, 575 (1999), astro-ph/9810256.
  - [4] B. Zhang and P. Meszaros, *Int.J.Mod.Phys. A* **19**, 2385 (2004), astro-ph/0311321.
  - [5] T. Piran, *Rev.Mod.Phys.* **76**, 1143 (2005), astro-ph/0405503.
  - [6] E. Nakar, *Phys.Rept.* **442**, 166 (2007), astro-ph/0701748.
  - [7] E. Berger, *New Astron.Rev.* **55**, 1 (2011), 1005.1068.
  - [8] L. Rezzolla, B. Giacomazzo, L. Baiotti, J. Granot, C. Kouveliotou, and M. A. Aloy, *Astrophys.J.* **732**, L6 (2011), 1101.4298.
  - [9] B. Abbott et al. (LIGO Scientific Collaboration), *Rept. Prog. Phys.* **72**, 076901 (2009), 0711.3041.
  - [10] LIGO, URL <http://www.ligo.caltech.edu>.
  - [11] F. Acernese et al., *J. Opt. A: Pure Appl. Opt.* **10**, 064009 (2008).
  - [12] VIRGO, URL <http://www.virgo.infn.it>.
  - [13] GEO 600, URL <http://www.geo600.org>.
  - [14] B. Schutz, *Class. Quantum Grav.* **16**, A131 (1999).
  - [15] P. C. Peters and J. Mathews, *Phys. Rev.* **131**, 435 (1963).
  - [16] P. C. Peters, *Phys. Rev.* **136**, B1224 (1964).
  - [17] A. G. Lyne et al., *Science* **303**, 1153 (2004), astro-ph/0401086.
  - [18] W. Tichy, *Phys. Rev.* **D84**, 024041 (2011), 1107.1440.
  - [19] S. Osłowski, T. Bulik, D. Gondek-Rosinska, and K. Belczynski, *Mon. Not. Roy. Astr. Soc.* **413**, 461 (2011), 0903.3538.
  - [20] P. Kiel, J. Hurley, M. Bailes, and J. Murray, *Mon. Not. Roy. Astr. Soc.* **388**, 393 (2008), 0805.0059.
  - [21] T. W. Baumgarte and S. L. Shapiro, *Phys. Rev.* **D80**, 064009 (2009), 0909.0952.
  - [22] T. W. Baumgarte and S. L. Shapiro, *Phys. Rev.* **D80**, 089901(E) (2009), 0909.0952.
  - [23] S. Bonazzola, E. Gourgoulhon, and J.-A. Marck, *Phys. Rev. Lett.* **82**, 892 (1999), gr-qc/9810072.
  - [24] E. Gourgoulhon, P. Grandclement, K. Taniguchi, J.-A. Marck, and S. Bonazzola, *Phys. Rev.* **D63**, 064029 (2001), gr-qc/0007028.
  - [25] P. Marronetti, G. J. Mathews, and J. R. Wilson, *Phys. Rev.* **D60**, 087301 (1999), arXiv:gr-qc/9906088.
  - [26] K. Uryu and Y. Eriguchi, *Phys. Rev.* **D61**, 124023 (2000), gr-qc/9908059.
  - [27] P. Marronetti and S. L. Shapiro, *Phys. Rev.* **D68**, 104024 (2003), gr-qc/0306075.
  - [28] K. Taniguchi and E. Gourgoulhon, *Phys. Rev.* **D66**, 104019 (2002), gr-qc/0207098.
  - [29] K. Taniguchi and E. Gourgoulhon, *Phys. Rev.* **D68**, 124025 (2003), gr-qc/0309045.
  - [30] K. Uryu, F. Limousin, J. L. Friedman, E. Gourgoulhon, and M. Shibata, *Phys. Rev. Lett.* **97**, 171101 (2006), gr-qc/0511136.
  - [31] K. Uryu, F. Limousin, J. L. Friedman, E. Gourgoulhon, and M. Shibata, *Phys. Rev.* **D80**, 124004 (2009), 0908.0579.
  - [32] W. Tichy, *Phys. Rev.* **D74**, 084005 (2006), gr-qc/0609087.
  - [33] W. Tichy, *Class. Quant. Grav.* **26**, 175018 (2009), 0908.0620.
  - [34] W. Tichy, *Phys. Rev.* **D80**, 104034 (2009), 0911.0973.
  - [35] C. W. Misner, K. S. Thorne, and J. A. Wheeler, *Gravitation* (W. H. Freeman, San Francisco, 1973).
  - [36] G. Schäfer and N. Wex, *Physics Lett. A* **174**, 196 (1993).
  - [37] W. Tichy, B. Brügmann, M. Campanelli, and P. Diener, *Phys. Rev.* **D67**, 064008 (2003), gr-qc/0207011.
  - [38] W. Tichy, B. Brügmann, and P. Laguna, *Phys. Rev.* **D68**, 064008 (2003), gr-qc/0306020.
  - [39] W. Tichy and B. Brügmann, *Phys. Rev. D* **69**, 024006 (2004), gr-qc/0307027.
  - [40] L. Bildsten and C. Cutler, *Astrophys. J.* **400**, 175 (1992).